| | | | | | |
|---|---|---|---|---|---|
| Iguchi Y, Katsuno M, Ikenaka K, Ishigaki S, Sobue G. | Amyotrophic lateral sclerosis: an update on recent genetic insights. | J Neurol. | 260 | 2917-27 | 2013 |
| Takagi S, Iguchi Y, Katsuno M, Ishigaki S, Ikenaka K, Fujioka Y, Honda D, Niwa J, Tanaka F, Watanabe H, Adachi H, Sobue G. | RNP2 of RNA recognition motif 1 plays a central role in the aberrant modification of TDP-43. | PLoS One. | 8 | e66966 | 2013 |
| Honda D, Ishigaki S, Iguchi Y, Fujioka Y, Udagawa T, Masuda A, Ohno K, Katsuno M, Sobue G. | The ALS/FTLD-related RNA-binding proteins TDP-43 and FUS have common downstream RNA targets in cortical neurons. | FEBS Open Bio. | 4 | 1-10 | 2013 |
| Fujioka Y, Ishigaki S, Masuda A, Iguchi Y, Udagawa T, Watanabe H, Katsuno M, Ohno K, Sobue G. | FUS-regulated region- and cell-type-specific transcriptome is associated with cell selectivity in ALS/FTLD. | Sci Rep. | 3 | 2388 | 2013 |
| Multiple-System Atrophy Research Collaboration. | Mutations in COQ2 in familial and sporadic multiple-system atrophy. | N Engl J Med. | 369 | 233-44 | 2013 |
| Doi H, Adachi H, Katsuno M, Minamiyama M, Matsumoto S, Kondo N, Miyazaki Y, Iida M, Tohnai G, Qiang Q, Tanaka F, Yanagawa T, Warabi E, Ishii T, Sobue G. | p62/SQSTM1 differentially removes the toxic mutant androgen receptor via autophagy and inclusion formation in a spinal and bulbar muscular atrophy mouse model | J Neurosci. | 33 | 7710-27 | 2013 |
| Ikenaka K, Kawai K, Katsuno M, Huang Z, Jiang YM, Iguchi Y, Kobayashi K, Kimata T, Waza M, Tanaka F, Mori I, Sobue G. | dnc-1/dynactin 1 knockdown disrupts transport of autophagosomes and induces motor neuron degeneration. | PLoS One. | 8 | e54511 | 2013 |

| | | | | | |
|---|---|---|---|---|---|
| Kondo N, Katsuno M, Adachi H, Minamiyama M, Doi H, Matsumoto S, Miyazaki Y, Iida M, Tohnai G, Nakatsuji H, Ishigaki S, Fujioka Y, Watanabe H, Tanaka F, Nakai A, Sobue G. | Heat shock factor-1 influences pathological lesion distribution of polyglutamine-induced neurodegeneration. | Nat Commun. | 4 | 1405 | 2013 |
| Tsuiji H, Iguchi Y, Furuya A, Kataoka A, Hatsuta H, Atsuta N, Tanaka F, Hashizume Y, Akatsu H, Murayama S, Sobue G, Yamanaka K. | Spliceosome integrity is defective in the motor neuron diseases ALS and SMA. | EMBO Mol Med. | 5 | 221-34 | 2013 |
| Nakamura R, Atsuta N, Watanabe H, Hirakawa A, Watanabe H, Ito M, Senda J, Katsuno M, Tanaka F, Izumi Y, Morita M, Ogaki K, Taniguchi A, Aiba I, Mizoguchi K, Okamoto K, Hasegawa K, Aoki M, Kawata A, Abe K, Oda M, Konagaya M, Imai T, Nakagawa M, Tsuji S, Kaji R, Nakano I, Sobue G. | Neck weakness is a potent prognostic factor in sporadic amyotrophic lateral sclerosis patients. | J Neurol Neurosurg Psychiatry. | 84 | 1365-71 | 2013 |
| Rabkin J, Ogino M, Goetz R, McElhiney M, Marziliano A, Imai T, Atsuta N, Morita M, Tateishi T, Matsumura T, Mitsumoto H. | Tracheostomy with invasive ventilation for ALS patients: neurologists' roles in the US and Japan. | Amyotroph Lateral Scler Frontotemporal Degener. | 14 | 116-23 | 2013 |
| Iguchi Y, Katsuno M, Niwa J, Takagi S, Ishigaki S, Ikenaka K, Kawai K, Watanabe H, Yamanaka K, Takahashi R, Misawa H, Sasaki S, Tanaka F, Sobue G. | Loss of TDP-43 causes age-dependent progressive motor neuron degeneration. | Brain | 136 | 1371-82 | 2013 |

# Ⅳ．研究成果の刊行物・別刷

# Evaluation of *SLC20A2* mutations that cause idiopathic basal ganglia calcification in Japan

Megumi Yamada, MD*
Masaki Tanaka, MD*
Mari Takagi, BA
Seiju Kobayashi, MD, PhD
Yoshiharu Taguchi, MD, PhD
Shutaro Takashima, MD, PhD
Kortaro Tanaka, MD, PhD
Tetsuo Touge, MD, PhD
Hiroyuki Hatsuta, MD
Shigeo Murayama, MD, PhD
Yuichi Hayashi, MD, PhD
Masayuki Kaneko, PhD
Hiroyuki Ishiura, MD, PhD
Jun Mitsui, MD, PhD
Naoki Atsuta, MD, PhD
Gen Sobue, MD, PhD
Nobuyuki Shimozawa, MD, PhD
Takashi Inuzuka, MD, PhD
Shoji Tsuji, MD, PhD
Isao Hozumi, MD, PhD

Correspondence to
Dr. Hozumi:
hozumi@gifu-pu.ac.jp

## ABSTRACT

**Objective:** To investigate the clinical, genetic, and neuroradiologic presentations of idiopathic basal ganglia calcification (IBGC) in a nationwide study in Japan.

**Methods:** We documented clinical and neuroimaging data of a total of 69 subjects including 23 subjects from 10 families and 46 subjects in sporadic cases of IBGC in Japan. Mutational analysis of *SLC20A2* was performed.

**Results:** Six new mutations in *SLC20A2* were found in patients with IBGC: 4 missense mutations, 1 nonsense mutation, and 1 frameshift mutation. Four of them were familial cases and 2 were sporadic cases in our survey. The frequency of families with mutations in *SLC20A2* in Japan was 50%, which was as high as in a previous report on other regions. The clinical features varied widely among the patients with *SLC20A2* mutations. However, 2 distinct families have the same mutation of S637R in *SLC20A2* and they have similar characteristics in the clinical course, symptoms, neurologic findings, and neuroimaging. In our study, all the patients with *SLC20A2* mutations showed calcification. In familial cases, there were symptomatic and asymptomatic patients in the same family.

**Conclusion:** *SLC20A2* mutations are a major cause of familial IBGC in Japan. The members in the families with the same mutation had similar patterns of calcification in the brain and the affected members showed similar clinical manifestations. *Neurology*® 2014;82:1-8

## GLOSSARY

**DNTC** = diffuse neurofibrillary tangles with calcification; **FIBGC** = familial idiopathic basal ganglia calcification; **IBGC** = idiopathic basal ganglia calcification; **MMSE** = Mini-Mental State Examination; **PDGF** = platelet-derived growth factor; **PDGFRB** = platelet-derived growth factor receptor-$\beta$; **Pi** = inorganic phosphate; **PiB** = Pittsburgh compound B; **PiT** = type III sodium-dependent phosphate transporter; **PKC** = paroxysmal kinesigenic choreoathetosis.

Idiopathic basal ganglia calcification (IBGC), also known as Fahr disease, is thought to be a rare neuropsychiatric disorder characterized by symmetrical calcification in the basal ganglia and other brain regions. Clinical manifestations range widely from asymptomatic to variable symptoms including headaches, psychosis, and dementia.[1] The diagnosis of IBGC generally relies on the visualization of bilateral calcification mainly in the basal ganglia by neuroimaging and the absence of metabolic, infectious, toxic, or traumatic causes.[2,3]

The mode of inheritance of familial IBGC (FIBGC) has been thought to be autosomal dominant and, to date, 4 responsible chromosomal regions have been identified, namely 14q (IBGC1), 2q37 (IBGC2), 8p11.21 (IBGC3), and 5q32 (IBGC4).[3–14] The causative gene at the IBGC3 locus was identified as *SLC20A2* encoding type III sodium-dependent phosphate transporter 2 (PiT-2). Screening of a large series of patients with IBGC revealed that mutations in *SLC20A2* are a major cause of FIBGC[10]; moreover, other mutations in *SLC20A2* have recently been reported in China and Brazil.[11–13] The mutations of *PDGFRB* encoding platelet-derived growth factor

**Supplemental data at
www.neurology.org**

(PDGF) receptor-β (PDGFRB) and *PDGFB* have recently been reported to cause calcification in the brain.[14,15]

We have collected clinical information of patients with IBGC in a nationwide survey in Japan. Here, on the basis of a mutational analysis of *SLC20A2*, we aim to establish the molecular epidemiology of IBGC3 and evaluate clinically and genetically *SLC20A2* mutations in Japan.

**METHODS** **Subjects and samples.** We collected clinical information on patients with IBGC in a nationwide study. The criteria for the selection of patients in the initial survey were as follows: 1) conspicuous calcification is observed in the basal ganglia and/or dentate nucleus by CT scan; 2) calcification is bilateral and symmetrical; and 3) idiopathic (absence of biochemical abnormalities, and an infectious, toxic, or traumatic cause).[2,3] Neurologists enrolled patients in the survey. They examined the medical charts and performed the neurologic examinations again if necessary. The survey was approved by the Ethics Committee of the Gifu University Graduate School of Medicine. During the survey, some patients were found to have hypoparathyroidism, Aicardi-Goutières syndrome, and Cockayne syndrome, and these patients were excluded. For the genetic study, a total of 69 subjects from 41 hospitals provided written informed consent and were enrolled in the project. Of these patients, 46 came from families with a single affected member, and the other 23 came from 10 families with multiple affected members. We defined the former as sporadic patients and the latter as familial patients. The patients' mean age ± SD was 41.3 ± 23.6 years at registration. The patients comprised 32 males and 37 females.

**Standard protocol approvals, registrations, and patient consents.** All experiments on human DNA were approved by the Ethics Committees of both Gifu University and the University of Tokyo. After written informed consent was obtained, peripheral blood samples were collected.

**Mutational analysis.** Genomic DNA was extracted from the whole blood samples. *SLC20A2* analysis was performed by Sanger sequencing of all coding regions, as described in detail in e-Methods and table e-1, A and B, on the *Neurology*® Web site at www.

neurology.org. The pathologic potential of the identified variants was predicted using PolyPhen-2 (http://genetics.bwh.harvard.edu/pph/).[16]

**RESULTS** **Mutational analysis.** We screened a total of 69 subjects including 23 subjects from 10 families in which multiple affected subjects were observed and 46 subjects in sporadic cases, all of whom were Japanese. Six new mutations in *SLC20A2* were found: 4 missense mutations, 1 nonsense mutation, and 1 frameshift mutation (figure 1). Electropherograms showed the individual heterozygous mutations (figure e-1). None of them were present in an in-house exome sequencing data set (358 Japanese control subjects), dbSNP 137 (www.ncbi.nlm.nih.gov/snp/), or the National Heart, Lung, and Blood Institute "Grand Opportunity" Exome Sequencing Project (ESP6500SI-V2). In silico analysis predicted deleterious consequences, as determined from the residue changes in figures 1 and e-1. When confined to the FIBGC patients, 5 of the 10 families (50.0%) showed mutations in *SLC20A2*. In contrast, 2 of the 46 patients (4.3%) with sporadic IBGC carried mutations in *SLC20A2* in this study.

**Clinical manifestations.** The clinical manifestations are summarized in table 1. A positive family history of IBGC was present in 5 families. Families 1 and 2 had the same mutation.

**Familial cases.** *Case 1 (in family 1).* The proband in family 1 was a 64-year-old woman who had dysarthria and gait disturbance for 5 years. She showed no dementia. Her neurologic examination revealed dysarthria, small steppage gait, rigidity at bilateral wrist joints, bradykinesia, and a pyramidal sign. Her CT images revealed severe calcification at the bilateral globus pallidus, caudate nuclei, thalamus, subcortical white matter, and dentate nuclei (figure 2C). Her son's CT showed similar brain calcification (figure 2D), although he was clinically asymptomatic. His DNA study revealed the

---

Figure 1    Schematic representation of causative mutations in *SLC20A2* in idiopathic basal ganglia calcification
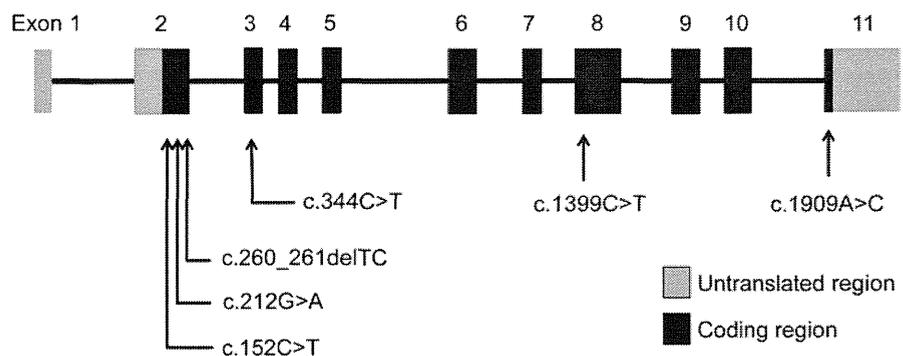


Six new causative mutations in exon 2 (c.152C>T, c.212 G>A, c.260_261delTC), exon 3 (c.344C>T), exon 8 (c.1399C>T), and exon 11 (c.1909A>C) were found in this study.

- 42 -

**Table 1** Clinical features of 6 individuals (probands) with *SLC20A2* mutations

|  | Case 1 | Case 2 | Case 3 | Case 4 | Case 5 | Case 6 | Case 7 |
|---|---|---|---|---|---|---|---|
| Mutation | c.1909A>C | c.1909A>C | c.344C>T | c.212G>A | c.1399C>T | c.152C>T | c.260_261delTC |
|  | S637R | S637R | T115M | R71H | R467X | A51V | L87Hfs*6 |
| Zygosity | Hetero | Hetero | Hetero | Hetero | Hetero | Hetero | Hetero |
| Exon | 11 | 11 | 3 | 2 | 8 | 2 | 2 |
| **Proband information** | | | | | | | |
| Age at detection of calcification, y | 60 | 51 | 60 | 73 | 23 | 71 | 74 |
| Age at onset, y | 58 | 50 | 60 | 71 | 15 | 71 | 57 |
| Onset symptom | Dysarthria | Dysarthria | Dementia | Parkinsonism | PKC | Dementia | Athetosis |
| Neurologic findings | | | | | | | |
| Cognitive impairment (MMSE) | 27 | 24 | 20 | 16 | 30 | 22 | 22 |
| Pyramidal sign | + | + | − | − | − | − | − |
| Extrapyramidal sign | + | + | − | + | − | − | + |
| **Family information (except the proband)** | | | | | | | |
| No. of other individuals with calcification | 1 | 2 | 5 | 1 | 1 | 0[a] | 0[a] |
| No. of other individuals with confirmed mutations | 1 | NE | 5 | NE | 1 | NA | NA |
| No. of other symptomatic individuals | 0 | 0 | 2 | 0 | 0 | NA | NA |
| Other symptoms (no.) in the family | — | — | Mental disorder (1), alcoholism (1) | — | — | NA | NA |

Abbreviations: MMSE = Mini-Mental State Examination; NA = not applicable; NE = not examined; PKC = paroxysmal kinesigenic choreoathetosis.
[a] Because there was no other family member who had any neurologic symptoms, brain CT screening of other family members was not performed.

same mutation in exon 11 that had been found in his mother.

*Case 2 (in family 2).* The proband in family 2 was a 54-year-old woman who had dysarthria and gait disturbance for 4 years. She showed mild mental deterioration in Mini-Mental State Examination (MMSE) score of 24 points, frontal signs, dysarthria, mild parkinsonism (rigidity of bilateral wrist joints and bradykinesia), adiadochokinesis, spasticity, and small steppage gait. Her CT images revealed severe calcification at the bilateral globus pallidus, caudate nuclei, thalamus, subcortical white matter, and dentate nuclei (figure 2E). Although her son and cousin also showed calcification in CT images, they were asymptomatic. Her DNA analysis revealed the same mutation as that in family 1.

*Case 3 and other symptomatic individuals (in family 3).* The proband was a 69-year-old woman (II-1 in the pedigree in figure 3). She was admitted to a hospital at the age of 65 because of forgetfulness since the age of 60 years. Her MMSE score was 20, which indicated a possibility of dementia (MMSE score below 22). Decreased blood flow was detected in the bilateral basal ganglia and thalamus and the right frontal lobe in particular by SPECT. She had a positive family history of brain calcification, as shown in figure 3A. The initial clinical diagnosis had been diffuse neurofibrillary tangles with calcification (DNTC),[17]

although to our knowledge familial cases of DNTC have not been reported. Her son had psychological disorders including violent behavior; unfortunately, no brain CT had yet been performed on him. In the patients in family 3, the degree of calcification was mild compared with that observed in the other families (figure 3, B–G). Her brother with calcification in the brain (II-7) had a mental disorder and another (II-8) presented with alcoholism. The 3 other relatives with calcification were asymptomatic (II-5, II-9, and III-3). The symptomatic patients (II-1, II-7, and II-8) showed more apparent brain atrophy than the others (figure 3, B, D, and E, respectively). The individuals with calcification on the CT images (II-1, II-5, II-7, II-8, II-9, and III-3) had the same mutation in exon 3 in *SLC20A2*. However, the individuals with no calcification (III-2, III-5, and IV-1) revealed no mutation in *SLC20A2*. In summary, 6 patients had calcification among the 10 individuals examined by CT scan in family 3 and all of them carrying the *SLC20A2* mutation exhibited similar calcification on CT images. However, persons without the mutation did not show calcification.

*Case 4 (in family 4).* Family 4 had a mutation in exon 2. The proband developed clumsiness of her hands and gait unsteadiness at the age of 71 years, and she was diagnosed as having Parkinson disease. Visual

- 43 -

**Figure 2    CT images and family trees of families 1 and 2**
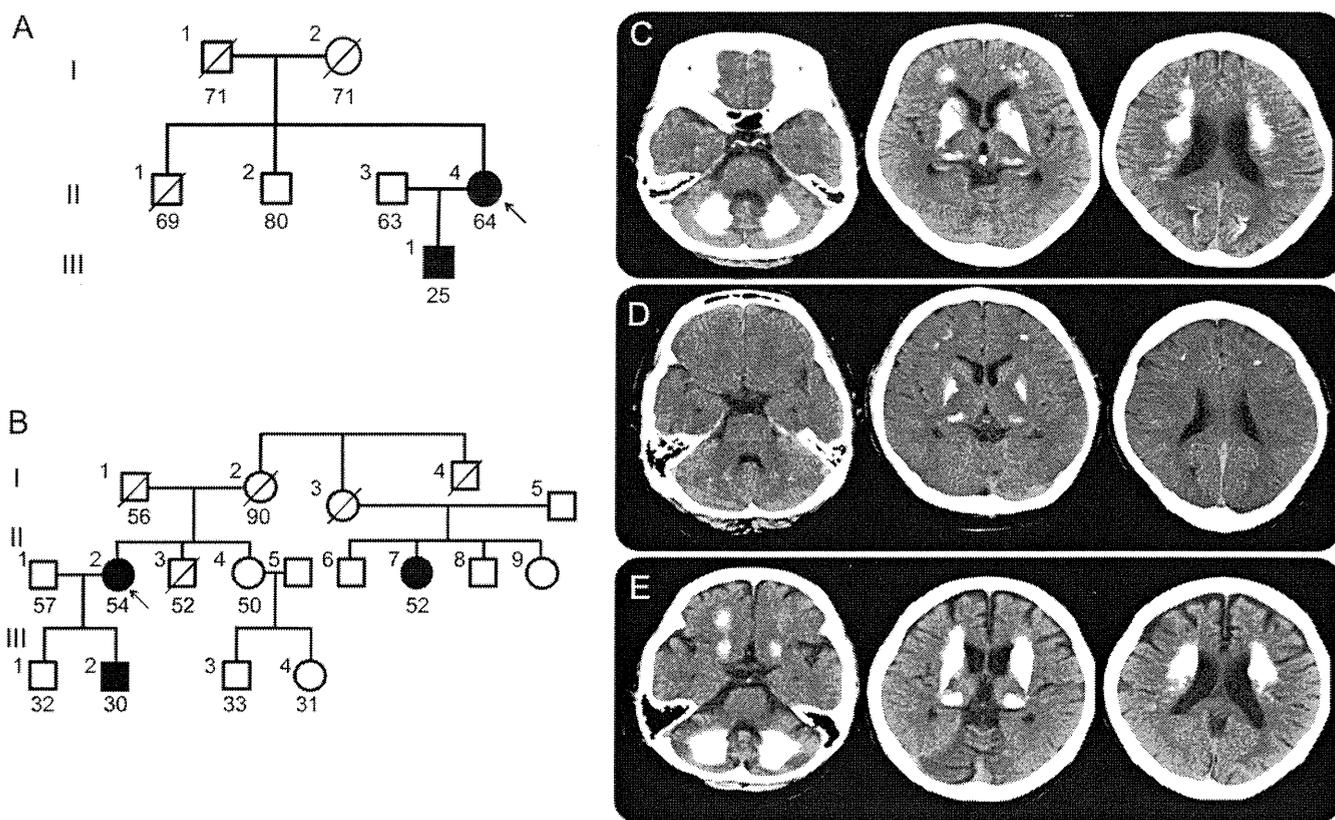
(A) Family tree of family 1. (B) Family tree of family 2. The arrow indicates the index subject. Filled symbols represent patients affected by brain calcification. We show the ages of persons under symbols in the family tree for those we could obtain. (C) CT images of proband (II-4 in pedigree of family 1, part A). (D) CT images of the proband's son (III-1 in pedigree of family 1, part A). (E) CT images of the proband (II-2 in pedigree of family 2, part B). All have mutation of S637R.

hallucinations started with the initiation of medication. She showed parkinsonism (rigidity, bradykinesia, and postural instability), which responded to levodopa. Her MMSE score was 16. Her brain CT images revealed calcification at the globus pallidus, caudate nuclei, and dentate nuclei, and her daughter, who was asymptomatic, also had intracranial calcification (figure e-2C). Brain CT was not performed in her other children. Her SPECT images showed decreased perfusion in the bilateral frontal, temporal, and parietal regions of the brain. She died of pneumonia at the age of 79. Neuropathologic examination revealed neuronal loss and Lewy bodies in the substantia nigra, locus ceruleus, amygdala, and parahippocampal gyrus indicative of Parkinson disease, and prominent deposition of calcium in the parenchyma and the wall of arteries in the globus pallidum and dentate nuclei compatible with the pathologic findings of IBGC.

*Case 5 (in family 5).* The proband was a 24-year-old man who had paroxysmal kinesigenic choreoathetosis (PKC). His laboratory data were normal except for CT findings. He presented with an attack of PKC after exercise and his symptom responded well to carbamazepine. His CT images revealed calcification at

the globus pallidus, thalamus, subcortical white matter, and dentate nuclei (figure e-2B [A]). We had an opportunity to examine his parents, who had no symptoms or signs. Mutational analysis of *SLC20A2* of his parents with their informed consent revealed the same mutation in exon 8 in his mother as he had. Brain CT scan of his mother confirmed calcification at the globus pallidus, subcortical white matter, and dentate nuclei.

**Sporadic cases.** *Case 6.* The patient had a mutation in exon 2. She was a 72-year-old woman who noticed forgetfulness at the age of 71. She had no motor deficits. Her MMSE score was 22, and her score on the revised Hasegawa Dementia Scale was 24. Her Frontal Assessment Battery score at bedside was 5, indicating a frontal lobe deficit (cutoff score, 11/12). The index scores of the revised Wechsler Memory Scale were as follows: attention and concentration, 86; verbal memory, 89; general memory, 85; attention/concentration, 71; and delayed recall, 75. Her brain CT images revealed calcification at the globus pallidus, caudate nuclei, thalamus, subcortical and periventricular white matter, and dentate nuclei (figure e-2B [B]). Her SPECT images showed decreased perfusion in the left frontal,

4        Neurology 82    February 25, 2014
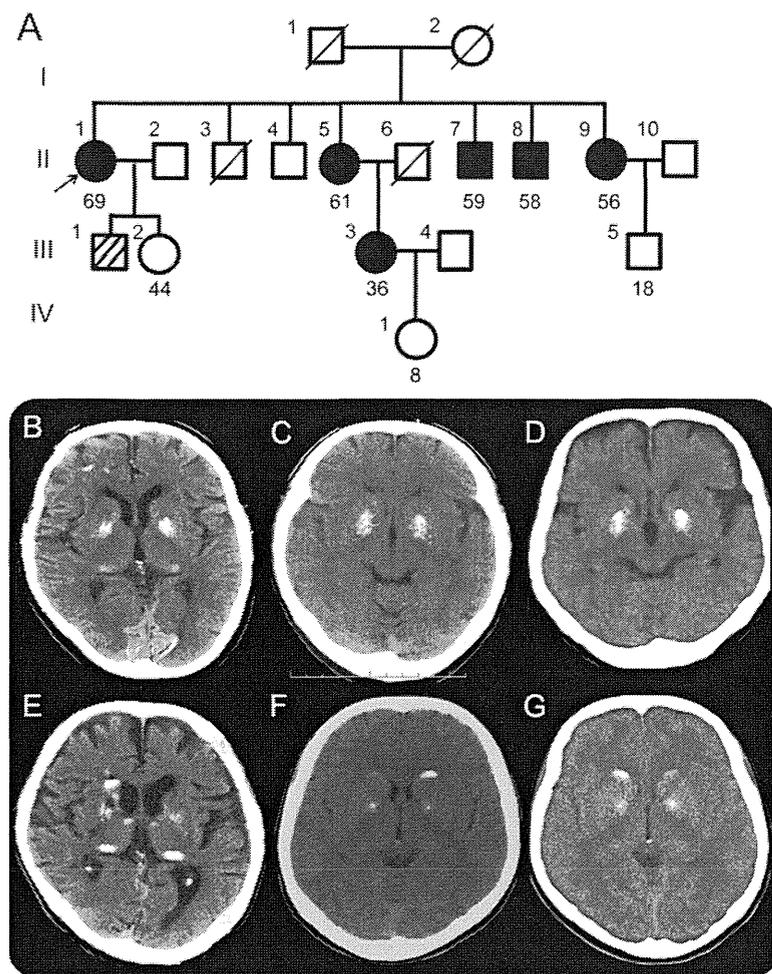
(A) Pedigree of family 3. The arrow indicates the index subject. Filled symbols represent patients affected by brain calcification. We show the ages of persons under symbols in the family tree for those we could obtain. The striped symbol represents a symptomatic patient, although his CT image and DNA sample were not available for the study. (B) CT image of the proband (II-1 in pedigree of family 3). (C) CT image of asymptomatic II-5. (D) CT image of symptomatic II-7. (E) CT image of symptomatic II-8. (F) CT image of asymptomatic II-9. (G) CT image of asymptomatic III-3. All have mutation of T115M.

subcortical and periventricular white matter, and dentate nuclei (figure e-2B [C]). His SPECT images showed decreased perfusion in the bilateral (predominantly in the left) frontal and temporal regions of the cerebrum and bilateral cerebellum. [$^{11}$C]PiB retention was not observed by [$^{11}$C]PiB PET, which was performed at the age of 81. There were no other family members presenting with similar neurologic symptoms. CT scan was not performed for other individuals in the family.

**DISCUSSION** We have obtained clinical information of 161 patients with brain calcification in a nationwide study. We discovered that 3 patients had hypoparathyroidism, Aicardi-Goutières syndrome, and Cockayne syndrome during the survey. CT images revealed varying degrees of calcification, from marked calcification in the basal ganglia to patchy calcification in various regions, suggesting diversity in the etiologies. Some patients were incidentally found to have calcification by CT performed for head injury caused by accidents. Because our previous survey revealed a considerable frequency (1%–2%) of patchy calcification in the CT images of all patients in 2 university hospitals in Japan,[18] more asymptomatic IBGC patients with patchy calcification may exist than the number that we had previously assumed to be present in the population in Japan. After the examination by neurologists, we collected 69 DNA samples from patients who met the criteria for IBGC.[2,3] Symptoms and neurologic findings varied widely from asymptomatic to variable symptoms including headaches, psychosis, and dementia.

In this study, we investigated mutations in *SLC20A2* in 69 patients with IBGC in Japan and identified 4 new mutations in 10 familial cases (the same mutation in 2 families) and 2 other new mutations in 46 sporadic cases. The frequency of families with mutations in *SLC20A2* was 50% (5 of the 10 families), and that of sporadic patients was 4.3% (2 of the 46 patients). The frequency of the mutations in *SLC20A2* in FIBGC in Japan was as high as in other countries in a previous report.[10] Case 5 indicates that it is difficult to reliably determine sporadic cases without brain CT scans and genetic studies of all members in the family.

The mutations in our study existed in exons 2, 3, 8, and 11. One of these mutations (R467X) in exon 8 resulted in a substitution to a TGA stop codon, and the other (c.260_261delTC) in exon 2 was a frameshift. None of the mutations were reported previously, indicating heterogeneities of the mutations in *SLC20A2*. Taken together with other reports, causative mutations identified in *SLC20A2* include 6 mutations in exon 2, 1 in exon 3, 3 in exon 4, 1 in exon 5, 1 in exon 7, 10 in exon 8, 2 in exon 9, 4 in exon 10, and 4 in exon 11.[9–12] It does not seem that there

temporal, and parietal regions of the cerebrum and bilateral cerebellum. [$^{11}$C] Pittsburgh compound B (PiB) retention was not observed by [$^{11}$C]PiB PET. There were no other family members presenting with similar neurologic symptoms. CT scan was not performed for other individuals in the family.

*Case 7.* The patient was a 78-year-old man who had a frameshift in exon 2. Involuntary movement of the left thumb and index finger like "pill-rolling" began in his sixth decade. His family first noticed memory impairment at the age of 75. Gait disturbance appeared at the age of 77 and oral dyskinesia and left shoulder shrugging appeared at the age of 78. His scores on the MMSE and Frontal Assessment Battery were 22 and 10, respectively. His brain CT images showed calcification at the globus pallidus, thalamus,

- 45 -

are mutation hot spots in *SLC20A2*. The in silico analysis using PolyPhen-2 for the missense mutations predicted all to be likely damaging, as determined from the residue changes. We drew the structure model of the PiT-2 protein using the TOPO2 software (http://www.sacs.ucsf.edu/TOPO/top.html). The schematic structure of the PiT-2 protein with the mutations is shown in figure 4.

Although the clinical features varied widely among the families with IBGC with *SLC20A2* mutations, the patients in families 1 and 2 with the same *SLC20A2* mutation exhibited similar clinical manifestations including dysarthria, mild cognitive decline, pyramidal signs, and extrapyramidal signs as well as similar ages at detection of calcification and onset of symptoms. Of note, the CT images among the affected individuals in the 2 families are similar (figure 2). In family 3, in contrast, 3 symptomatic patients presented with dementia, psychological disorder, and alcoholism, accompanied with brain atrophy in CT images. None of them showed movement disorders such as those in families 1 and 2.

Although mutational analysis and CT scan were not performed in other familial members of cases 6 and 7, concordance of the presence of mutations of *SLC20A2* and brain calcification were confirmed in 15 individuals, and we did not observe any individuals who carried the mutation and did not show brain calcification. These observations strongly support a high penetrance of the *SLC20A2* mutations regarding brain calcification.

Correlations of genotypes and neurologic phenotypes, however, have been controversial. *SLC20A2* mutations in patients with FIBGC have been

described to show variability in clinical manifestations among the families. In the present study, the 2 affected individuals in families 1 and 2, who carried the same mutation, exhibited quite similar neurologic manifestations and clinical courses, suggesting a genotype-phenotype correlation of the S637R mutation. Of note, 2 individuals aged 56 and 61 years in family 3 did not exhibit any neurologic manifestations despite carrying the mutation and having brain calcification, indicating that penetrance regarding the neurologic manifestations is incomplete.

In case 4, interestingly, the proband showed pathologic findings of both IBGC and Parkinson disease. Because Parkinson disease is a common disorder in aged people, there remains a possibility that the presence of IBGC and Parkinson disease is coincidental.

Case 5 had a mutation that leads to a premature stop codon, making an incomplete structure of PiT-2. His neurologic symptom was PKC controllable by carbamazepine. Intriguingly, several patients with IBGC have been reported to present with PKC or paroxysmal nonkinesigenic dyskinesia.[19,20] For these cases of PKC or paroxysmal nonkinesigenic dyskinesia, mutational analyses of not only *SLC20A2* but also *PRRT2* and MRI will be indispensable.[21,22]

Herein, we have reported 5 cases of FIBGC and 2 cases of IBGC with *SLC20A2* mutations in Japan. We could not find any characteristic features of Japanese patients, although we had discovered that each case has a new mutation in *SLC20A2*, respectively.

The mechanisms of calcification and cell damage remain to be elucidated. Despite that the expression of PiT-2 encoded by *SLC20A2* is distributed widely in the human body,[23] mutations in *SLC20A2* cause

**Figure 4     Schematic structure of PiT-2 (type III sodium-dependent phosphate transporter) with the mutations**

- 46 -
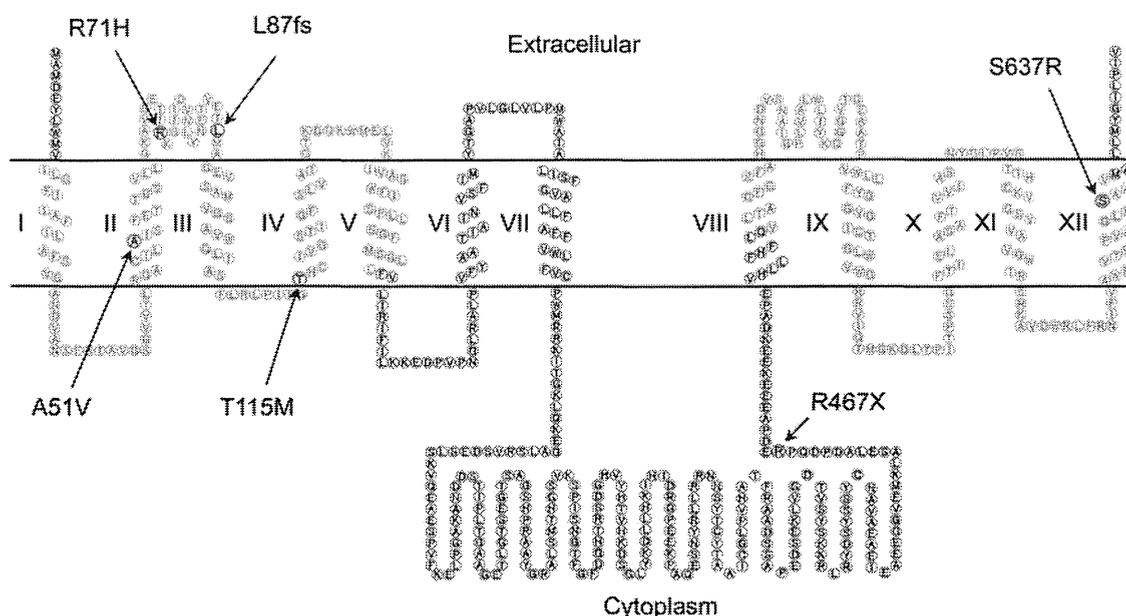
calcification only in the brain. Mutations in *SLC34A2* have been reported to cause pulmonary alveolar microlithiasis.[24] Because Npt2b encoded by *SLC34A2* is the only phosphate transporter that is highly expressed in the lungs,[25] the mutations in *SLC34A2* are compatible with the lesion of the alveolar type II cells in the lungs.[24] Because the limitation of calcification to the brain cannot be explained by only the mutation in *SLC20A2* followed by abnormalities of inorganic phosphate (Pi) transport via PiT-2, there might be some other genes responsible for calcification in the brain, or the mutations in *SLC20A2* may take some toxic gain of function. The dysfunction of Pi transport can explain the accumulation of various metals in regions of the brain and the abnormal distribution of metals, which we observed in CSF[26] and hair in the patients with IBGC.[27] We have recently shown that PiT-2 immunopositivity was expressed predominantly in neurons, astrocytes, and vascular endothelial cells in the mouse brain.[28] PDGF-B is expressed in endothelial cells and neurons.[29] PDGF-B homodimer (PDGF-BB) enhanced the expression of PiT-1 mRNA encoded by *SLC20A1* in human aortic smooth muscle cells.[30] The hypomorph of PDGF-B in mice has recently been revealed to cause brain calcification through pericyte and blood-brain barrier impairment.[15] Recently, simple knockout of *SLC20A2* has also been shown to lead to calcification in the mouse brain.[31] PiT-2, PDGF, and as yet undetermined other molecules are considered to have pivotal roles in blood vessel–associated calcification and neuronal death in patients with IBGC. Elucidation of the molecular basis underlying IBGC will contribute to the development of therapeutic measures for patients with calcification in the brain.

## AUTHOR CONTRIBUTIONS

Principal investigator: Isao Hozumi. Study supervision: Shoji Tsuji, Gen Sobue, Takashi Inuzuka, and Kortaro Tanaka. Manuscript draft preparation: Megumi Yamada and Masaki Tanaka. Acquisition and collection of data: Seiju Kobayashi, Yoshiharu Taguchi, Shutaro Takashima, Tetsuo Touge, Hiroyuki Hatsuta, and Shigeo Murayama. Analysis and interpretation: Megumi Yamada, Masaki Tanaka, Mari Takagi, Yuichi Hayashi, Masayuki Kaneko, Naoki Atsuta, Nobuyuki Shimozawa, Hiroyuki Ishiura, and Jun Mitsui.

## ACKNOWLEDGMENT

## STUDY FUNDING

## DISCLOSURE

## REFERENCES

1. Manyam BV. What is and what is not "Fahr's disease." Parkinsonism Relat Disord 2005;11:73–80.

- 47 -

2. Bonazza S, La Morgia C, Martinelli P, Capellari S. Strio-pallido-dentate calcinosis: a diagnostic approach in adult patients. Neurol Sci 2011;32:537–545.

3. Sobrido MJ, Hopfer S, Geschwind DH. Familial idiopathic basal ganglia calcification. In: GeneReviews NCBI Bookshelf [online]. Available at: http://www.ncbi.nlm.nih.gov/books/NBK1421/. Accessed March 1, 2013.

4. Geschwind DH, Loginov M, Stern JM. Identification of a locus on chromosome 14q for idiopathic basal ganglia calcification (Fahr disease). Am J Hum Genet 1999;65:764–772.

5. Lemos RR, Oliveira DF, Zatz M, Oliveira JR. Population and computational analysis of the MGEA6 P521A variation as a risk factor for familial idiopathic basal ganglia calcification (Fahr's disease). J Mol Neurosci 2011;43:333–336.

6. Oliveira JR, Spiteri E, Sobrido MJ, et al. Genetic heterogeneity in familial idiopathic basal ganglia calcification (Fahr disease). Neurology 2004;63:2165–2167.

7. Volpato CB, De Grandi A, Buffone E, et al. 2q37 as a susceptibility locus for idiopathic basal ganglia calcification (IBGC) in a large South Tyrolean family. J Mol Neurosci 2009;39:346–353.

8. Dai X, Gao Y, Xu Z, et al. Identification of a novel genetic locus on chromosome 8p21.1-q11.23 for idiopathic basal ganglia calcification. Am J Med Genet B Neuropsychiatr Genet 2010;7:1305–1310.

9. Wang C, Li Y, Shi L, et al. Mutations in SLC20A2 link familial idiopathic basal ganglia calcification with phosphate homeostasis. Nat Genet 2012;44:254–256.

10. Hsu SC, Sears RL, Lemos RR, et al. Mutations in SLC20A2 are a major cause of familial idiopathic basal ganglia calcification. Neurogenetics 2013;14:11–22.

11. Zhang Y, Guo X, Wu A, et al. Association between a novel mutation in SLC20A2 and familial idiopathic basal ganglia calcification. PLoS One 2013;8:e57060.

12. Lemos RR, Oliveira MF, Oliveira JR. Reporting a new mutation at the SLC20A2 gene in familial idiopathic basal ganglia calcification. Eur J Neurol 2013;20:e43–e44.

13. Nicolas G, Pottier C, Maltête D, et al. Mutation of the PDGFRB gene as a cause of idiopathic basal ganglia calcification. Neurology 2013;80:181–187.

14. Chen WJ, Yao XP, Zhang QJ, et al. Novel SLC20A2 mutations identified in southern Chinese patients with idiopathic basal ganglia calcification. Gene 2013;529:159–162.

15. Keller A, Westenberger A, Sobrido MJ, et al. Mutations in the gene encoding PDGF-B cause brain calcifications in humans and mice. Nat Genet 2013;45:1077–1082.

16. Adzhubei IA, Schmidt S, Peshkin L. A method and server for predicting damaging missense mutations. Nat Methods 2010;7:248–249.

17. Kosaka K. Diffuse neurofibrillary tangles with calcification: a new presenile dementia. J Neurol Neurosurg Psychiatry 1994;57:594–596.

18. Yamada M, Asano T, Okamoto K, et al. High frequency of calcification in basal ganglia on brain computed tomography images in Japanese older adults. Geriatr Gerontol Int 2013;13:706–710.

19. Chung AJ, Cho G, Kim SJ. A case of paroxysmal kinesigenic dyskinesia in idiopathic bilateral striopallidodentate calcinosis. Seizure 2012;21:802–804.

20. Alemdar M, Selek A, Iseri P, Efendi H, Komsuoğlu SS. Fahr's disease presenting with paroxysmal non-kinesigenic dyskinesia: a case report. Parkinsonism Relat Disord 2008;14:69–71.

21. Chen WJ, Lin Y, Xiong ZQ, et al. Exome sequencing identifies truncating mutations in PRRT2 that cause paroxysmal kinesigenic dyskinesia. Nat Genet 2011;43:1252–1255.

22. Fabbri M, Marini C, Bisulli F, et al. Clinical and polygraphic study of familial paroxysmal kinesigenic dyskinesia with PRRT2 mutation. Epileptic Disord 2013;15:123–127.

23. Lederer E, Miyamoto K. Clinical consequences of mutations in sodium phosphate cotransporters. Clin J Am Soc Nephrol 2012;7:1179–1187.

24. Feild JA, Zhang L, Brun KA, Brooks DP, Edwards RM. Cloning and functional characterization of a sodium-dependent prostate transporter expressed in human lung and small intestine. Biochem Biophys Res Commun 1999;258:578–582.

25. Huqun, Izumi S, Miyazawa H, et al. Mutations in the SLC34A2 gene are associated with pulmonary alveolar microlithiasis. Am J Respir Crit Care Med 2007;175:263–268.

26. Hozumi I, Kohmura A, Kimura A, et al. High levels of copper, zinc, iron and magnesium, but not calcium, in the cerebrospinal fluid of patients with Fahr's disease. Case Rep Neurol 2010;2:46–51.

27. Takagi M, Ozawa K, Yasuda H, et al. Decreased bioelements content in the hair of patients with Fahr's disease (idiopathic bilateral calcification in the brain). Biol Trace Elem Res 2013;159:9–13.

28. Inden M, Iriyama M, Takagi M, et al. Localization of type-III sodium-dependent phosphate transporter 2 in the mouse brain. Brain Res 2013;1531:75–83.

29. Andrae J, Gallini R, Betsholtz C. Role of platelet-derived growth factors in physiology and medicine. Genes Dev 2008;22:1276–1312.

30. Giachelli CM, Jono S, Shioi A, et al. Vascular calcification and inorganic phosphate. Am J Kidney Dis 2001;38(4 suppl 1):S34–S37.

31. Jensen N, Schrøder HD, Hejbøl EK, et al. Loss of function of Slc20a2 associated with familial idiopathic basal ganglia calcification in humans causes brain calcifications in mice. J Mol Neurosci 2013;51:994–999.

- 48 -

Original Investigation

# Lower Motor Neuron Involvement in TAR DNA-Binding Protein of 43 kDa–Related Frontotemporal Lobar Degeneration and Amyotrophic Lateral Sclerosis

Yuichi Riku, MD; Hirohisa Watanabe, MD; Mari Yoshida, MD; Shinsui Tatsumi, MD; Maya Mimuro, MD; Yasushi Iwasaki, MD; Masahisa Katsuno, MD; Yohei Iguchi, MD; Michihito Masuda, MD; Jo Senda, MD; Shinsuke Ishigaki, MD; Tsuyoshi Udagawa, PhD; Gen Sobue, MD

**IMPORTANCE** TAR DNA-binding protein of 43 kDa (TDP-43) plays a major role in the pathogenesis of frontotemporal lobar degeneration (FTLD) and amyotrophic lateral sclerosis (ALS). Although a pathological continuity between FTLD and ALS has been suggested, the neuropathological changes of the lower motor neuron (LMN) systems have not been assessed in TDP-43–associated FTLD (FTLD-TDP), to our knowledge.

**OBJECTIVE** To investigate a pathological continuity between FTLD-TDP and ALS by comparing their respective neuropathological changes in the motor neuron system.

**DESIGN AND SETTING** A retrospective clinical medical record review and a semiquantitative neuropathological evaluation of the cranial motor nerve nuclei and spinal cord were conducted at autopsy. We included 43 patients with sporadic FTLD-TDP, type A, B, or C, from 269 consecutively autopsied patients with TDP-43 proteinopathy. Patients were categorized as having FTLD without ALS, FTLD-ALS (onset of FTLD symptoms/signs preceded those of ALS), or ALS-FTLD (onset of ALS symptoms/signs preceded those of FTLD).

**MAIN OUTCOMES AND MEASURES** Neuronal TDP-43 pathological changes and neuronal loss.

**RESULTS** Forty-three patients were included in the clinical analysis, and 29 from whom spinal cords were obtained were included in the neuropathological analysis. Survival time was significantly shorter in the FTLD-ALS and ALS-FTLD groups than in the FTLD without ALS group ($P < .001$). At neuropathological examination, 89% of patients in the FTLD without ALS group showed aggregations of TDP-43 in the spinal motor neurons. The LMN loss was most severe in ALS-FTLD, followed by FTLD-ALS and FTLD without ALS. All the patients with type A or C FTLD-TDP were included in the FTLD without ALS group, and all those with type B pathological changes were in the FTLD-ALS or the ALS-FTLD group. Lower motor neuron loss and TDP-43–positive skeinlike inclusions were observed in all pathological subtypes.

**CONCLUSIONS AND RELEVANCE** The LMN systems of FTLD-TDP frequently exhibit neuropathological changes corresponding to ALS. Thus, a pathological continuity between FTLD-TDP and ALS is supported at the level of the LMN system.

Supplemental content at
jamaneurology.com

**Author Affiliations:** Department of Neurology, Nagoya University Graduate School of Medicine, Nagoya, Japan (Riku, Watanabe, Katsuno, Iguchi, Masuda, Senda, Ishigaki, Udagawa, Sobue); Institute for Medical Science of Aging, Aichi Medical University, Aichi, Japan (Yoshida, Tatsumi, Mimuro, Iwasaki).

**Corresponding Author:** Gen Sobue, MD, Department of Neurology, Nagoya University Graduate School of Medicine, Tsurumai 65, Showa-ku, Nagoya, Japan (sobueg@med.nagoya-u.ac.jp).

Frontotemporal lobar degeneration (FTLD) is a sporadic or familial neurodegenerative disease that clinically encompasses frontotemporal dementia, language disorder, and motor symptoms.[1] Immunohistochemical profiles show that approximately half of patients with FTLD present with tau-positive disease, but the other half primarily exhibit an accumulation of TAR DNA-binding protein of 43 kDa (TDP-43), referred to as FTLD-TDP.[2-5] Currently, the cortical TDP-43 pathological changes in sporadic FTLD-TDP are classified into 3 subtypes: A, B, and C.[6-8]

TAR DNA-binding protein of 43 kDa is also a major disease protein in amyotrophic lateral sclerosis (ALS), which is characterized by upper motor neuron and lower motor neuron (LMN) involvement.[9] The pathological features of LMN involvement in ALS include neuronal loss, gliosis, TDP-43-positive neuronal inclusions with skeinlike or round shapes and glial inclusions, and Bunina bodies.[10]

Some patients exhibit symptoms of both ALS and FTLD, and the cerebral cortices of patients with FTLD and ALS almost always show type B TDP-43 changes.[7,11-13] Thus, a pathological continuity between FTLD and ALS has been proposed based on brain TDP-43 pathological findings. Studies of the cerebral cortex, including the motor cortex, and subcortical gray matter have shown common TDP-43 pathological findings in FTLD, FTLD with ALS, and ALS.[12,14-17] However, the neuropathological features of LMN systems in FTLD-TDP have not been investigated comprehensively, particularly in the spinal cord, although characterization of these features is necessary to confirm the pathological relationship between FTLD and ALS.

In this study, we investigated LMN pathological findings in patients with sporadic FTLD-TDP who clinically demonstrated FTLD, FTLD with ALS, or ALS. We also investigated the correlation between TDP-43 pathological subtypes (type A, B, and C) and LMN involvement to further elucidate the continuity of FTLD and ALS.

## Methods

### Study Patients

We enrolled 269 consecutively autopsied patients with sporadic and adult-onset FTLD, FTLD with ALS, or ALS in which pathological aggregation of TDP-43 was confirmed at the Department of Neuropathology, Institute for Medical Science of Aging, Aichi Medical University, from 1988 to 2012. All patients had been clinically evaluated by neurological experts in the affiliated hospitals of Nagoya University School of Medicine or Aichi Medical University. Permission to perform an autopsy and archive the nervous system tissues for research purposes was obtained from family members after death. The clinical data on the included patients were obtained from case notes made at diagnosis and at an advanced stage of illness. We initially excluded 216 of the 269 patients because they did not present clinical FTLD symptoms. In 53 patients, FTLD or FTLD with ALS was diagnosed according to the diagnostic criteria of FTLD and ALS.[1,18] Moreover, we subclassified FTLD with ALS into FTLD-ALS

(onset of FTLD symptoms/signs preceded those of ALS) and ALS-FTLD (onset of ALS symptoms/signs preceded those of FTLD) groups.

The enrolled patients were categorized into 3 groups: FTLD without ALS, FTLD-ALS, and ALS-FTLD. The FTLD symptoms were categorized into 2 groups: behavior-variant frontotemporal dementia and language impairments.[14] The LMN symptoms/signs were defined by progressive muscular weakness, muscular atrophy, fasciculation, or electromyographic findings. We excluded patients with Alzheimer disease-associated neurofibrillary pathological abnormalities that were more advanced than Braak stage IV,[19] those with argyrophilic grain disease, and those with invalid clinical data. Finally, 43 patients were included in the clinical analysis (11 with FTLD without ALS, 9 with FTLD-ALS, and 23 with ALS-FTLD). For comparison, we prepared 13 age-matched controls (mean [SD] age at death, 68.2 [6.9] years) who had no diagnosis of any neurodegenerative disease, dementia, or cerebrovascular disease.

### Clinical Analyses

The information regarding sex, age at onset, disease duration, and duration between onset of FTLD and ALS was collected from clinical notes. Causes of death were classified as respiratory failure due to respiratory muscle weakness, pneumonia, or other. The last category comprised systemic diseases other than respiratory failure or pneumonia, including cancer, ileus, infections, and renal failure. Information on the subtypes of dementia, clinical data on motor symptoms, and electromyographic results were also collected.

### Pathological Evaluations

For the neuropathological analysis, we excluded patients who had received a respirator/tracheotomy (n = 11) or whose spinal cord was not available (n = 3). In total, 29 patients were included in the neuropathological analysis and divided into 3 groups: FTLD without ALS (n = 9), FTLD-ALS (n = 8), and ALS-FTLD (n = 12). The tissues were fixed in 20% neutral-buffered formalin. The paraffin-embedded tissue blocks were cut at a thickness of 4.5 μm. We evaluated sections from the spinal cord and whole brain. The whole spinal cord was examined at each segmental level, but only the cervical cord was available in 3 patients and the sacral cord was not available in another 3.

For routine neuropathological examinations, the sections were stained with hematoxylin-eosin and Klüver-Barrera. Immunohistochemical studies were performed using a standard polymer-based method with the EnVision Kit or anti-goat immunoglobulin (Dako). As primary antibodies, we used antibodies to the following: anti-ubiquitin (ubiquitin, monoclonal mouse, 1:250; Millipore), anti-TDP-43 (TARDBP, polyclonal rabbit, 1:2500; ProteinTech), anti-phosphorylated TDP-43 (pTDP-43 ser409/410, polyclonal rabbit, 1:2500; CosmoBio), anti-phosphorylated tau (AT-8, monoclonal mouse, 1:4000; Innogenetics), anti-β-amyloid (β-amyloid 6F/3D, monoclonal mouse, 1:100; Dako), anti-CD68 (CD68, monoclonal mouse, 1:200; Dako), anti-cystatin C (cystatin C, polyclonal rabbit, 1:200; Dako), p62 N-terminal (p62N, polyclonal

- 50 -

guinea pig, 1:100; Progen), anti-ubiquilin 2 (UBQLN-2 5F5, monoclonal mouse, 1:5000; Abnova), and anti-choline acetyltransferase (ChAT, polyclonal goat, 1:100; Millipore). Diaminobenzidine (Wako) was used as the chromogen.

Antigens were retrieved with trypsin for anti-CD68 immunohistochemistry and with 95°C 3 mmol/L citrate buffer at 95°C for 20 minutes, followed by 5-minute incubation in 98% formic acid for anti-p62N, anti-TDP-43, anti-pTDP-43, and anti-ChAT immunohistochemistry. To confirm the presence of TDP-43-positive inclusions within the cholinergic motor neurons, we performed double immunohistochemistry using anti-pTDP-43 and anti-ChAT antibodies. Spinal cord specimens were prepared from 3 patients with type A, 3 with type B, and 2 with type C. Initially, the specimens were immunostained with the anti-ChAT and anti-goat immunoglobulin antibodies and diaminobenzidine. The anti-ChAT antibody was inactivated in distilled water at 100°C for 20 minutes, followed by immunohistochemistry with pTDP-43 and violet pigmentation using a VIP Peroxidase Substrate Kit (SK-4600; Vector).

For the semiquantitative neuropathological analysis, 2 investigators (Y.R. and M.Y.) observed the specimens containing the facial and hypoglossal nuclei and the anterior horn of the spinal cord. They evaluated the severity of LMN neuropathological changes that are indicative of ALS (neuronal loss, gliosis, aggregation of macrophages, TDP-43-immunopositive neuronal inclusions, and Bunina bodies) and graded neuronal loss and gliosis using Klüver-Barrera and hematoxylin-eosin staining. The investigators also evaluated the aggregations of macrophages rather than rod-shaped microglia using anti-CD68 immunohistochemistry and identified Bunina bodies using hematoxylin-eosin staining and anti-cystatin C immunohistochemistry. They scored the severity of neuronal loss and gliosis as grade 0 (none), 1 (mild), 2 (moderate), or 3 (severe) (eFigure 1 in Supplement. The appearance of TDP-43-positive inclusions was scored as grade 0 (none), grade 1 (1-5 neuronal inclusions per 5 fields; ×20 objective), grade 2 (6-10 inclusions), or grade 3 (≥11 inclusions) using anti-pTDP-43 immunohistochemistry.

Pathological cortical TDP-43 subtypes were identified according to current neuropathological criteria, using specimens from the frontal lobes, temporal lobes, and hippocampus.[5] For FTLD-TDP, type A was defined as the presence of neuronal cytoplasmic inclusions predominantly in the neocortex layer 2 and short dystrophic neurites; type B, as a predominance of neuronal cytoplasmic inclusions in all cortical layers; and type C, as a predominance of long dystrophic neurites in layer 2 and cytoplasmic inclusions in the dentate granular cells of the hippocampus. Our patient series did not include type D, which is characterized by numerous short dystrophic neurites and neuronal intranuclear inclusions in association with valosin-containing protein gene mutations. We also evaluated pathological changes in the upper motor neuron systems that include the primary motor cortex and corticospinal tract (CST). We evaluated the presence or absence of neuronal loss and gliosis in the primary motor cortex and myelin pallor, as well as the aggregation of macrophages in the CST.

## Immunohistochemical Screening of Hexanucleotide Repeat Expansion Sequence in Chromosome 9 Open Reading Frame 72

Our study focused on sporadic FTLD-TDP, and patients with familial histories of FTLD or ALS, dementia, or other neurodegenerative diseases were excluded. However, FTLD or ALS associated with chromosome 9 open reading frame 72 (C9ORF72) hexanucleotide expansion exhibits pathological aggregation of TDP-43 and, in some cases, low penetration,[20,21] although these mutations are extremely rare in Japan.[22] It was recently reported that the pattern of ubiquilin abnormalities in ALS and FTLD corresponds well with the presence of C9ORF72 hexanucleotide expansion.[23] The UBQLN-2-positive, p62-positive, but TDP-43-negative thick dystrophic neurites are abundantly present in patients with C9ORF72 hexanucleotide expansion, predominantly in the hippocampus and cerebellum. Because the materials for a genetic study were not available for a large proportion of our patients, we histologically screened C9ORF72 hexanucleotide expansion with the absence of UBQLN-2 and p62N-positive thick dystrophic neurites in the temporal lobes and cerebella of all patients.

## Statistical Analysis

The Mann-Whitney test was applied to continuous variables between 2 groups, and the Kruskal-Wallis test was applied to the analysis of continuous variables among 3 groups. The $\chi^2$ test was used for categorized variables among 3 groups. Spearman rank correlation coefficient analyses were applied to univariate correlations between the clinical groups and severity of pathological changes. Survival curves were constructed using the Kaplan-Meier method. The end point of clinical course was defined as death or the introduction of a respirator or tracheotomy. The significance level for all comparisons was set at $P < .05$. All statistical tests were 2 sided and were conducted using the PASW 18.0 program (IBM SPSS).

## Results

### Clinical Analysis

Patient characteristics are summarized in the **Table**. The mean (SD) time from symptom onset to death or respirator or tracheotomy administration was 50.5 (58.4) months across all patients. The survival time from symptom onset did not differ significantly between the FTLD-ALS and ALS-FTLD groups but was significantly shorter for the FTLD without ALS group than for the FTLD-ALS or ALS-FTLD group (**Figure 1** and Table; $P < .001$). The most common cause of death for the ALS-FTLD and FTLD-ALS groups was respiratory failure, but patients with FTLD without ALS commonly died of other systemic diseases ($P < .001$). Frequencies of dementia subtypes did not significantly differ between the clinical groups.

With regard to motor symptoms/signs, 3 patients in the FTLD without ALS group had hyperreflexia, 1 had the Babinski sign, and 1 had spasticity, but none had a clinical diagnosis of progressive lateral sclerosis (PLS) according to the published diagnostic criteria of PLS.[24] Patients with FTLD-ALS or

- 51 -

**Table. Clinical and Demographic Patient Characteristics**

| Characteristic | FTLD Without ALS (n = 11) | FTLD-ALS (n = 9) | ALS-FTLD (n = 23) | P Value |
|---|---|---|---|---|
| | | Patient Group | | |
| Sex, No. female/male[a] | 8/3 | 3/6 | 10/13 | .16 |
| Age at onset, mean (SD), y[b] | 62.4 (9.4) | 58.2 (11.3) | 61.2 (9.5) | .79 |
| Clinical duration without respirator or tracheotomy, median (range), mo[c] | 84.0 (47.0-360.0) | 28.0 (7.0-60.0) | 22.0 (7.0-71.0) | <.001 |
| Duration between FTLD and ALS, median (range), mo[d] | | 18.0 (4.0-48.0) | 19.0 (0-60.0) | .92 |
| Patients with tracheotomy, No. (%)[a] | 0 | 0 | 2 (9) | .40 |
| Patients with respirators, No. (%)[a] | 0 | 1 (11) | 8 (35) | .047 |
| Duration with respirator or tracheotomy, median (range), mo | | 30.0 | 39.0 (1.0-141.0) | ... |
| Causes of death, No. (%)[a] | | | | |
| Respiratory failure | 0 | 6 (67) | 20 (87) | <.001 |
| Pneumonia | 3 (27) | 3 (33) | 3 (13) | .37 |
| Other | 8 (73) | 0 | 0 | <.001 |
| Subtypes of dementia, No. (%) | | | | |
| Behavior-variant FTD | 7 (64) | 7 (78) | 19 (83) | .29 |
| Language impairments | 4 (36) | 2 (22) | 4 (17) | .62 |
| Motor symptoms/signs, No. (%) | | | | |
| Muscle weakness[a] | 0 | 9 (100) | 23 (100) | <.001 |
| Muscle atrophy | 0 | 7 (78) | 22 (96) | <.001 |
| Fasciculation | 0 | 4 (44) | 15 (65) | .002 |
| Hyperreflexia | 3 (27) | 5 (56) | 17 (74) | .009 |
| Babinski sign | 1 (9) | 4 (44) | 3 (13) | .08 |
| Spasticity | 1 (9) | 0 | 1 (4) | .63 |
| Electromyography, No. (%) | | | | |
| Total examined | 2 (18) | 4 (82) | 21 (91) | ... |
| Active denervation[a] | 0 | 3 (75) | 12 (57) | .054 |

Abbreviations: ALS, amyotrophic lateral sclerosis; ALS-FTLD, onset of ALS symptoms/signs preceding those of frontotemporal lobar degeneration (FTLD); ellipses, not significant; FTD, frontotemporal dementia; FTLD-ALS, onset of FTLD symptoms/signs preceding those of ALS.

[a] $\chi^2$ Test.

[b] Kruskal-Wallis test.

[c] Log-rank test.

[d] Mann-Whitney test.

ALS-FTLD generally exhibited both upper motor neuron and LMN symptoms/signs except for 3 who exhibited only LMN symptoms/signs. Based on the electromyographic data, active denervation potentials (positive sharp waves and fibrillation potentials[18]) were identified in 3 patients with FTLD-ALS and 12 with ALS-FTLD but not in any of those with FTLD without ALS.

## Pathological Evaluations of the LMN System

The results of semiquantitative pathological evaluations of the 3 clinical groups are summarized in **Figure 2.** In the FTLD without ALS group, 8 of 9 patients (89%) showed pTDP-43-positive neuronal inclusions. In addition, neuronal loss and gliosis in the spinal anterior horns were observed in 5 of 11 patients (45%) and Bunina bodies were present in 4 (36%). The pathological changes in LMN systems were most severe in the ALS-FTLD group, followed by the FTLD-ALS group, and were rather mild in the FTLD without ALS group. Among control patients, 1 had a pTDP-43-positive glial inclusion in the lumbar anterior horn, but this patient did not show neuronal loss, gliosis, or Bunina bodies (eFigure 2 in Supplement).

**Figure 1. Survival by Clinical Group**
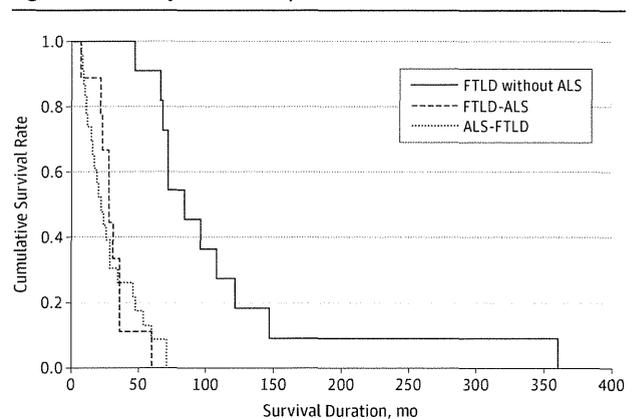


Kaplan-Meier plot showing the survival rates of patients with frontotemporal lobar degeneration (FTLD) without amyotrophic lateral sclerosis (ALS) (solid line; n = 11), those in whom the onset of FTLD symptoms/signs preceded those of ALS (FTLD-ALS) (dashed line; n = 9), and those in whom the onset of ALS symptoms/signs preceded those of FTLD (ALS-FTLD) (dotted line; n = 23). Survival times were significantly shorter in patients with FTLD without ALS than in those with FTLD-ALS or ALS-FTLD (P < .001).

- 52 -

**Figure 2. Semiquantitative Evaluations of Pathological Changes by Clinical Group**

| Patients | FTLD Without ALS | | | | | | | | | FTLD-ALS | | | | | | | | ALS-FTLD | | | | | | | | | | | | P Values | r Values |
|---|---|---|---|---|---|---|---|---|---|---|---|---|---|---|---|---|---|---|---|---|---|---|---|---|---|---|---|---|---|---|---|
| | 1 | 2 | 3 | 4 | 5 | 6 | 7 | 8 | 9 | 10 | 11 | 12 | 13 | 14 | 15 | 16 | 17 | 18 | 19 | 20 | 21 | 22 | 23 | 24 | 25 | 26 | 27 | 28 | 29 | | |
| Clinical duration, mo | 47 | 66 | 84 | 108 | 147 | 360 | 68 | 96 | 122 | 22 | 23 | 28 | 28 | 31 | 36 | 36 | 60 | 7 | 8 | 9 | 10 | 16 | 20 | 22 | 24 | 26 | 54 | 60 | 71 | | |
| **Neuronal loss** | | | | | | | | | | | | | | | | | | | | | | | | | | | | | | | |
| Facial nuclei | + | - | - | - | + | - | - | - | - | ++ | NA | + | + | + | + | ++ | + | + | ++ | + | + | ++ | ++ | NA | ++ | + | +++ | + | | <.01 | 0.730 |
| Hypoglossal nuclei | - | - | - | - | - | - | - | - | - | +++ | NA | ++ | +++ | ++ | + | +++ | ++ | +++ | + | + | +++ | +++ | +++ | ++ | +++ | +++ | +++ | | <.01 | 0.823 |
| Anterior horn of Cx | + | ++ | - | - | + | - | - | - | + | ++ | ++ | + | ++ | ++ | + | ++ | + | +++ | ++ | ++ | ++ | ++ | ++ | NA | +++ | ++ | +++ | ++ | | <.01 | 0.804 |
| Anterior horn of Tx | + | + | NA | + | + | - | NA | - | + | + | ++ | ++ | ++ | ++ | ++ | + | ++ | ++ | + | +++ | ++ | ++ | +++ | ++ | ++ | +++ | +++ | ++ | | <.01 | 0.768 |
| Anterior horn of Lx | - | - | NA | + | + | - | NA | - | - | + | + | + | + | + | + | ++ | + | ++ | ++ | +++ | + | ++ | ++ | NA | ++ | +++ | ++ | ++ | ++ | <.01 | 0.856 |
| Anterior horn of Sx | - | - | NA | + | - | - | NA | - | - | + | NA | + | + | + | + | ++ | + | ++ | ++ | NA | NA | ++ | ++ | NA | ++ | ++ | +++ | NA | + | <.01 | 0.880 |
| **Gliosis** | | | | | | | | | | | | | | | | | | | | | | | | | | | | | | | |
| Facial nuclei | ++ | - | - | - | + | - | - | - | - | ++ | NA | + | + | + | + | ++ | + | ++ | ++ | + | ++ | ++ | ++ | NA | + | ++ | +++ | ++ | | <.01 | 0.768 |
| Hypoglossal nuclei | - | - | - | - | - | - | - | - | - | +++ | NA | ++ | ++ | ++ | + | +++ | ++ | +++ | + | + | +++ | +++ | +++ | ++ | +++ | +++ | +++ | ++ | | <.01 | 0.828 |
| Anterior horn of Cx | + | ++ | - | - | + | - | - | - | + | ++ | ++ | + | +++ | ++ | + | ++ | + | +++ | + | ++ | ++ | ++ | ++ | NA | +++ | ++ | +++ | | <.01 | 0.730 |
| Anterior horn of Tx | + | + | NA | - | + | - | NA | - | + | + | ++ | + | ++ | ++ | ++ | + | ++ | ++ | + | +++ | ++ | ++ | +++ | ++ | ++ | +++ | +++ | ++ | | <.01 | 0.740 |
| Anterior horn of Lx | - | - | NA | + | + | - | NA | - | - | + | + | + | ++ | + | + | ++ | + | ++ | ++ | +++ | ++ | ++ | ++ | NA | +++ | +++ | ++ | ++ | ++ | <.01 | 0.878 |
| Anterior horn of Sx | - | - | NA | + | - | - | NA | - | - | + | NA | + | ++ | + | + | ++ | + | ++ | ++ | NA | NA | ++ | ++ | NA | +++ | +++ | +++ | NA | ++ | <.01 | 0.904 |
| **pTDP-43-positive neuronal inclusions** | | | | | | | | | | | | | | | | | | | | | | | | | | | | | | | |
| Facial nuclei | + | - | - | - | + | - | - | - | - | ++ | NA | + | + | + | + | + | + | + | ++ | + | ++ | +++ | + | NA | + | ++ | + | + | ++ | <.01 | 0.729 |
| Hypoglossal nuclei | - | + | + | - | - | + | - | - | + | NA | + | + | + | + | ++ | + | + | - | + | +++ | + | - | + | + | - | + | + | | .08 | 0.348 |
| Anterior horn of Cx | + | + | + | + | + | - | + | + | ++ | ++ | + | + | + | + | + | + | ++ | ++ | +++ | + | +++ | ++ | ++ | NA | + | + | + | + | | <.01 | 0.511 |
| Anterior horn of Tx | + | + | NA | - | + | - | NA | + | + | + | + | ++ | + | + | + | + | + | + | + | ++ | + | ++ | + | + | + | + | + | + | | <.05 | 0.403 |
| Anterior horn of Lx | + | + | NA | + | - | - | NA | + | + | + | +++ | ++ | ++ | + | + | + | ++ | ++ | + | ++ | ++ | ++ | + | +++ | NA | + | + | + | ++ | <.05 | 0.412 |
| Anterior horn of Sx | + | - | NA | - | - | - | NA | - | + | ++ | NA | ++ | + | + | + | + | + | + | + | NA | NA | + | +++ | NA | - | + | + | NA | + | <.05 | 0.458 |
| **Aggregation of macrophages** | | | | | | | | | | | | | | | | | | | | | | | | | | | | | | | |
| Facial nuclei | ++ | - | + | - | + | - | - | - | - | ++ | NA | + | - | ++ | + | ++ | + | ++ | + | + | + | + | ++ | NA | + | ++ | ++ | + | + | <.01 | 0.518 |
| Hypoglossal nuclei | + | - | - | - | - | - | - | - | - | + | NA | - | + | ++ | + | + | - | +++ | + | ++ | + | + | +++ | - | ++ | +++ | + | ++ | - | <.01 | 0.634 |
| Anterior horn of Cx | + | + | - | + | + | - | - | + | + | ++ | + | + | + | ++ | + | ++ | ++ | + | + | + | - | ++ | NA | + | + | + | - | - | | 0.78 | 0.073 |
| Anterior horn of Tx | + | + | NA | - | - | - | NA | + | + | ++ | + | + | ++ | + | + | + | + | + | + | ++ | ++ | + | ++ | + | + | + | + | + | + | <.05 | 0.435 |
| Anterior horn of Lx | - | ++ | NA | + | - | - | NA | - | - | + | - | - | - | + | + | ++ | + | +++ | ++ | +++ | ++ | + | +++ | NA | + | +++ | ++ | ++ | ++ | <.01 | 0.721 |
| Anterior horn of Sx | - | + | NA | + | - | - | NA | - | - | + | NA | - | + | + | + | + | + | +++ | ++ | NA | NA | + | ++ | NA | + | +++ | ++ | NA | + | <.01 | 0.751 |
| Bunina bodies | + | + | + | - | + | - | - | - | - | + | + | + | + | + | + | + | - | + | + | + | + | + | + | + | - | + | + | + | + | | |
| Brain TDP-43 disease type | A | A | A | A | A | A | C | C | C | B | B | B | B | B | B | B | B | B | B | B | B | B | B | B | B | B | B | B | B | | |

Findings shown include the severity of neuronal loss, gliosis, phosphorylated TAR DNA-binding protein of 43 kDa (pTDP-43) pathological changes, and aggregations of macrophages and the presence of Bunina bodies in the lower motor neuron systems. The severity of each pathological change was graded as 0 (none [-, not colored]), 1 (mild [+, green]), 2 (moderate [++, yellow]), or 3 (severe [+++, red]). Neuropathological changes became increasingly severe in those in whom amyotrophic lateral sclerosis (ALS) symptoms/signs preceded those of frontotemporal lobar degeneration (FTLD; ALS-FTLD), as well as the FTLD-ALS (FTLD symptoms/signs preceding those of ALS) and FTLD without ALS groups (Spearman rank order). Cx indicates cervical cord; Lx, lumbar cord; NA, not assessed; Sx, sacral cord; TDP-43, TAR DNA-binding protein of 43 kDa; and Tx, thoracic cord.

According to cortical TDP-43 pathological findings,[5] 29 patients were classified into 3 subtypes: A (n = 6), B (n = 20), or C (n = 3). Patients with FTLD without ALS showed type A or C disease, whereas those with FTLD-ALS or ALS-FTLD all showed type B disease (Figure 2 and **Figure 3**). For all the subtypes, the LMN system showed neuropathological changes that were indicative of ALS, including pTDP-43-positive neuronal and glial inclusions, neuronal loss, and gliosis. In patients with type A disease (**Figure 4A-H**), the severity of neuronal loss and gliosis in LMN systems ranged from none to moderate. Five patients (83%) in this group had pTDP-43-positive, skeinlike cytoplasmic and/or nuclear inclusions (Figure 4B and C), and 4 (67%) had Bunina bodies (Figure 4E and F) in the LMNs.

All 20 patients in the type B group (Figure 4I-L) showed neuronal loss, gliosis, and pTDP-43-positive skeinlike cytoplasmic inclusions in the LMN systems, and 18 (90%) had Bunina bodies. Among the 3 patients with type C disease (Figure 4M-P), 1 (33%) had mild loss of the LMNs (Figure 4M), and all 3 (100%) had pTDP-43-positive skeinlike cytoplasmic inclusions in the LMNs (Figure 4N). Unlike patients with the other subtypes, those with type C disease lacked Bunina bodies. Moreover, thick dystrophic neurites were prominent in the spinal anterior horn in patients with type A or C disease but rarely present in those with type B disease (Figure 4G and O). These dystrophic neurites were larger in diameter (8-12 μm) than those found in the cortices. In a double immunohistochemical analysis, pTDP-43-positive inclusions were found within the cytoplasm of ChAT-positive neurons in patients with type A, B, and C disease (Figure 4H, L, and P).

## Pathological Evaluations of the Upper Motor Neuron System

In the primary motor cortex, neuronal loss and gliosis were evident in 5 patients with FTLD without ALS (56%), 2 with FTLD-ALS (25%), and 3 with ALS-FTLD (25%). Myelin pallor in the CST was evident in 6 patients with FTLD without ALS (67%), 1 with FTLD-ALS (12%), and 2 with ALS-FTLD (17%). Aggregations of macrophages in the CST were evident in 4 patients with FTLD without ALS (44%), 5 with FTLD-ALS (62%), and 6 with ALS-FTLD (50%).

Figure 3. Semimacroscopic Appearances and Brain Pathological Findings in Patients With Type A, B, and C Pathological Changes



Findings in patients with type A (A-D), B (E-H), and C (I-L) pathological changes. In a patient with type A pathological change, cerebral coronal sections showed cortical atrophy of the parasylvian region (A). Transverse section of the cervical cord showed marked myelin pallor in the corticospinal tract (B). Microscopically, the frontal cortices showed marked neuronal loss (C) and phosphorylated TAR DNA-binding protein of 43 kDa (pTDP-43)–positive neuronal inclusions and short dystrophic neurites (D). In a patient with type B pathological change, the cerebral cortex showed severe temporal atrophy (E), neuronal loss (G), and pTDP-43–positive neuronal inclusions (H). The corticospinal tract showed mild

myelin pallor (F). In a patient with type C patholgoical change, the frontal and temporal cortices showed severe atrophy (I), marked neuronal loss (K), and pTDP-43–positive long dystrophic neurites (L). The corticospinal tract showed marked myelin pallor (J). Klüver-Barrera staining (A, B, E, F, I, and J), hematoxylin-eosin staining (C, G, and K), and pTDP-43 immunohistochemistry (D, H, and L) were performed. Scale bars represent 1 cm (A, E, and I), 3 mm (B, F, and J), 100 μm (C, G, and K), and 20 μm (D, H, and L). Original magnifications are ×1 (A, B, E, F, I, and J), ×200 (C, G, and K), and ×400 (D, H, and L).

## Anti–UBQLN-2 and Anti–p62N Immunohistochemistry

No patients showed any cerebellar UBQLN-2–positive or p62N-positive structures. In the temporal lobes, UBQLN-2–positive structures were occasionally observed in 8 patients, but abundant, thick, and aggregatelike structures, which are found in patients with C9ORF72 expansions, were not observed (eFigure 3 in Supplement). We presumed that our patients did not have C9ORF72 expansions.

## Discussion

Our study demonstrated that pTDP-43–associated pathological changes were common in the spinal anterior horns of the FTLD without ALS, FTLD-ALS, and ALS-FTLD groups. Neuronal loss and gliosis were most severe among the ALS-FTLD group, followed by the FTLD-ALS and then the FTLD without ALS groups. Our results clearly demonstrated the pathological continuum among TDP-43–associated FTLD and ALS, even at the LMN level.

Although the FTLD without ALS group that lacked LMN symptoms showed a loss of LMNs, the degree of neuronal loss and TDP-43 disease were generally mild in this group. Experiment data using ALS mouse models revealed that symptoms developed when approximately 29% of spinal motor neurons were lost.[25] Further investigation will be needed to clarify whether LMN involvement occurs in a later stage of illness or progresses very slowly compared with cerebral involvement in FTLD without ALS.

Our results revealed that the FTLD-TDP types A, B, and C were associated with neuropathological changes corresponding to ALS in the spinal motor neurons. The severity of neuronal loss and pTDP-43 disease in the spinal motor neurons

may differ quantitatively among these neuropathological subtypes. Based on cortical TDP-43 pathological findings, patients in the type B group had severe neuronal loss and diffuse pTDP-43–positive neuronal inclusions, which were entirely identical to ALS, whereas these changes were mild in the type C group. In type A, LMN pathological findings were diverse regardless of clinical duration; their severity and extension may be heterogeneous among patients with type A disease, unlike those with type B or C disease. Indeed, type A disease has also been identified in the FTLD with ALS phenotype in sporadic or familial (C9ORF72 expansion or progranulin gene mutations) form.[2,5,21,26] Dystrophic neurites were prominent in the spinal anterior horn of patients with type A or C disease. In our patient series, Bunina bodies were observed in most patients with type A or B disease but were absent in those with type C disease, findings consistent with those of previous studies.[3,17]

Several studies have demonstrated that some patients with FTLD-TDP, particularly type C, showed marked CST degeneration.[3,11,17,27] We also observed a marked myelin pallor in the CST in 67% of patients with FTLD without ALS, 12% with FTLD-ALS, and 16% with ALS-FTLD (50% for type A, 15% for type B, and 100% for type C). Some patients showed neuronal loss or gliosis in the primary motor cortex to varying extents. Furthermore, patients with FTLD without ALS often exhibited severe degenerative changes in broad areas of the frontal cortices. The broad involvement of the frontal lobes might also contribute to the CST degeneration because CST fibers arise not only from the primary motor cortex but also from the premotor cortex and supplementary motor areas.[28]

Two limitations of our study is that the evaluation of slight or very mild muscle weakness was not completed and that there were few patients with electromyographic data in

- 54 -

Figure 4. Pathological Findings of Spinal Motor Neuron in Subtypes of TAR DNA-Binding Protein of 43 kDa (TDP-43) Pathological Changes
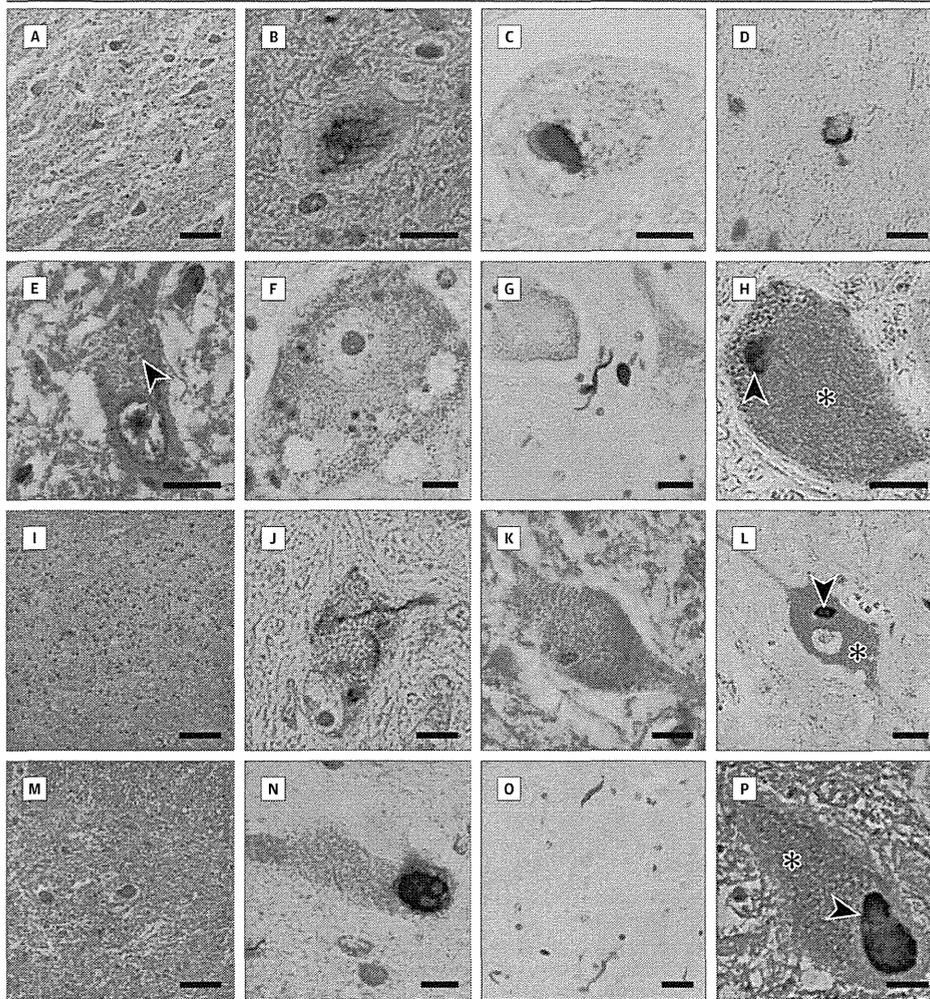


Patients with type A (A-H), type B (I-L), and type C (M-P) pathological changes. A patient with type A pathological change showed mild neuronal loss (A), phosphorylated TDP-43 (pTDP-43)–positive skeinlike cytoplasmic inclusions (B), nuclear inclusions (C), and glial inclusions (D), Bunina bodies (E [arrow] and F) in the spinal anterior horn, and dystrophic neurites (G). In a patient with type B pathological change, neuronal loss (I), pTDP-43–positive skeinlike cytoplasmic inclusions (J), and Bunina bodies (K) were markedly observed. In a patient with type C pathological change, the spinal anterior horn showed mild neuronal loss (M), pTDP-43–positive skeinlike cytoplasmic inclusions (N), and dystrophic neurites (O). Double immunohistochemistry for choline acetyltransferase (ChAT) and pTDP-43 revealed cytoplasmic inclusions (violet [arrows]) present within the cytoplasm of a ChAT-positive spinal motor neuron (brown [asterisks]) of patients with type A (H), B (L), or C (P) pathological change. Hematoxylin-eosin staining (A, E, I, K, and M), pTDP-43 immunohistochemistry (B, C, D, G, J, N, and O), cystatin-C (F), and double immunohistochemical analysis for pTDP-43 and ChAT (H, L, and P) were performed. Scale bars represent 100 (A, I, and M), 20 (G, L, and O), and 10 (B-F, H, J, K, N, and P) μm. Original magnifications are ×100 (A, I, and M), ×400 (G, L, and O), and ×1000 (B-F, H, J, K, N, and P).

the FTLD without ALS group. However, our clinical data demonstrated that patients with FTLD without ALS had significantly longer survival times than those with FTLD-ALS or ALS-FTLD. These prognostic data correspond well to previous results.[29,30] In addition, the causes of death differed considerably between the FTLD without ALS group and the FTLD-ALS and ALS-FTLD groups. Respiratory failure was observed in patients with FTLD-ALS or ALS-FTLD but not in those with FTLD without ALS, and respiratory failure was

strongly associated with severity of LMN loss. These results support the view that classification of FTLD based on the presence of LMN involvement was applicable in this study.

In conclusion, the LMN systems of FTLD-TDP generally show neuropathological changes that are indicative of ALS, although the severity of pathological changes differs among clinical phenotypes or subtypes of cortical TDP-43 disease. A pathological continuity between FTLD-TDP and ALS is supported by evidence of LMN involvement.

- 55 -

### REFERENCES

1. Cairns NJ, Neumann M, Bigio EH, et al. TDP-43 in familial and sporadic frontotemporal lobar degeneration with ubiquitin inclusions. *Am J Pathol.* 2007;171(1):227-240.

2. Josephs KA, Whitwell JL, Murray ME, et al. Corticospinal tract degeneration associated with TDP-43 type C pathology and semantic dementia. *Brain.* 2013;136(pt 2):455-470.

3. Mackenzie IR, Neumann M, Bigio EH, et al. Nomenclature and nosology for neuropathologic subtypes of frontotemporal lobar degeneration: an update. *Acta Neuropathol.* 2010;119(1):1-4.

4. Whitwell JL, Jack CR Jr, Parisi JE, et al. Does TDP-43 type confer a distinct pattern of atrophy in frontotemporal lobar degeneration? *Neurology.* 2010;75(24):2212-2220.

5. Mackenzie IR, Neumann M, Baborie A, et al. A harmonized classification system for FTLD-TDP pathology. *Acta Neuropathol.* 2011;122(1):111-113.

6. Mackenzie IR, Baborie A, Pickering-Brown S, et al. Heterogeneity of ubiquitin pathology in frontotemporal lobar degeneration: classification and relation to clinical phenotype. *Acta Neuropathol.* 2006;112(5):539-549.

7. Sampathu DM, Neumann M, Kwong LK, et al. Pathological heterogeneity of frontotemporal lobar degeneration with ubiquitin-positive inclusions delineated by ubiquitin immunohistochemistry and novel monoclonal antibodies. *Am J Pathol.* 2006;169(4):1343-1352.

8. Neumann M, Sampathu DM, Kwong LK, et al. Ubiquitinated TDP-43 in frontotemporal lobar degeneration and amyotrophic lateral sclerosis. *Science.* 2006;314(5796):130-133.

9. Josephs KA, Dickson DW. Frontotemporal lobar degeneration with upper motor neuron disease/primary lateral sclerosis. *Neurology.* 2007;69(18):1800-1801.

10. Geser F, Lee VM, Trojanowski JQ. Amyotrophic lateral sclerosis and frontotemporal lobar degeneration: a spectrum of TDP-43 proteinopathies. *Neuropathology.* 2010;30(2):103-112.

11. Snowden J, Neary D, Mann D. Frontotemporal lobar degeneration: clinical and pathological relationships. *Acta Neuropathol.* 2007;114(1):31-38.

12. Geser F, Martinez-Lage M, Robinson J, et al. Clinical and pathological continuum of multisystem TDP-43 proteinopathies. *Arch Neurol.* 2009;66(2):180-189.

13. Nishihira Y, Tan CF, Hoshi Y, et al. Sporadic amyotrophic lateral sclerosis of long duration is associated with relatively mild TDP-43 pathology. *Acta Neuropathol.* 2009;117(1):45-53.

14. Geser F, Stein B, Partain M, et al. Motor neuron disease clinically limited to the lower motor neuron is a diffuse TDP-43 proteinopathy. *Acta Neuropathol.* 2011;121(4):509-517.

15. Yoshida M. Amyotrophic lateral sclerosis with dementia: the clinicopathological spectrum. *Neuropathology.* 2004;24(1):87-102.

16. Kobayashi Z, Tsuchiya K, Arai T, et al. Clinicopathological characteristics of FTLD-TDP showing corticospinal tract degeneration but lacking lower motor neuron loss. *J Neurol Sci.* 2010;298(1-2):70-77.

17. Brooks BR, Miller RG, Swash M, Munsat TL; World Federation of Neurology Research Group on Motor Neuron Diseases. El Escorial revisited: revised criteria for the diagnosis of amyotrophic lateral sclerosis. *Amyotroph Lateral Scler Other Motor Neuron Disord.* 2000;1(5):293-299.

18. Neary D, Snowden JS, Gustafson L, et al. Frontotemporal lobar degeneration: a consensus on clinical diagnostic criteria. *Neurology.* 1998;51(6):1546-1554.

19. Braak H, Alafuzoff I, Arzberger T, Kretzschmar H, Del Tredici K. Staging of Alzheimer disease-associated neurofibrillary pathology using paraffin sections and immunocytochemistry. *Acta Neuropathol.* 2006;112(4):389-404.

20. Simón-Sánchez J, Dopper EG, Cohn-Hokke PE, et al. The clinical and pathological phenotype of C9ORF72 hexanucleotide repeat expansions. *Brain.* 2012;135(pt 3):723-735.

21. Murray ME, DeJesus-Hernandez M, Rutherford NJ, et al. Clinical and neuropathologic heterogeneity of c9FTD/ALS associated with hexanucleotide repeat expansion in C9ORF72. *Acta Neuropathol.* 2011;122(6):673-690.

22. Konno T, Shiga A, Tsujino A, et al. Japanese amyotrophic lateral sclerosis patients with GGGGCC hexanucleotide repeat expansion in C9ORF72. *J Neurol Neurosurg Psychiatry.* 2013;84(4):398-401.

23. Brettschneider J, Van Deerlin VM, Robinson JL, et al. Pattern of ubiquilin pathology in ALS and FTLD indicates presence of C9ORF72 hexanucleotide expansion. *Acta Neuropathol.* 2012;123(6):825-839.

24. Pringle CE, Hudson AJ, Munoz DG, Kiernan JA, Brown WF, Ebers GC. Primary lateral sclerosis. Clinical features, neuropathology and diagnostic criteria. *Brain.* 1992;115(pt 2):495-520.

25. Morrison BM, Janssen WG, Gordon JW, Morrison JH. Time course of neuropathology in the spinal cord of G86R superoxide dismutase transgenic mice. *J Comp Neurol.* 1998;391(1):64-77.

26. Baker M, Mackenzie IR, Pickering-Brown SM, et al. Mutations in progranulin cause tau-negative frontotemporal dementia linked to chromosome 17. *Nature.* 2006;442(7105):916-919.

27. Yokota O, Tsuchiya K, Arai T, et al. Clinicopathological characterization of Pick's disease versus frontotemporal lobar degeneration with ubiquitin/TDP-43-positive inclusions. *Acta Neuropathol.* 2009;117(4):429-444.

28. Standring S, ed. *Gray's Anatomy: The Anatomical Basis of Clinical Practice.* 39th edition. London, England: Churchill Livingstone; 2004.

29. Josephs KA, Knopman DS, Whitwell JL, et al. Survival in two variants of tau-negative frontotemporal lobar degeneration: FTLD-U vs FTLD-MND. *Neurology.* 2005;65(4):645-647.

30. Hodges JR, Davies R, Xuereb J, Kril J, Halliday G. Survival in frontotemporal dementia. *Neurology.* 2003;61(3):349-354.

- 56 -

REPORT

# ERBB4 Mutations that Disrupt the Neuregulin-ErbB4 Pathway Cause Amyotrophic Lateral Sclerosis Type 19

Yuji Takahashi,[1] Yoko Fukuda,[1] Jun Yoshimura,[2] Atsushi Toyoda,[3] Kari Kurppa,[4,5] Hiroyoko Moritoyo,[6] Veronique V. Belzil,[7] Patrick A. Dion,[7,8] Koichiro Higasa,[2] Koichiro Doi,[2] Hiroyuki Ishiura,[1] Jun Mitsui,[1] Hidetoshi Date,[1] Budrul Ahsan,[1] Takashi Matsukawa,[1] Yaeko Ichikawa,[1] Takashi Moritoyo,[6] Mayumi Ikoma,[9] Tsukasa Hashimoto,[9] Fumiharu Kimura,[10] Shigeo Murayama,[11] Osamu Onodera,[12] Masatoyo Nishizawa,[12] Mari Yoshida,[13] Naoki Atsuta,[14] Gen Sobue,[14] JaCALS,[15] Jennifer A. Fifita,[16,17,18] Kelly L. Williams,[16,17,18] Ian P. Blair,[16,17,18] Garth A. Nicholson,[16,17] Paloma Gonzalez-Perez,[19] Robert H. Brown, Jr.,[19] Masahiro Nomoto,[6] Klaus Elenius,[4,20] Guy A. Rouleau,[7,21,22] Asao Fujiyama,[3] Shinichi Morishita,[2] Jun Goto,[1] and Shoji Tsuji[1,23,*]

Amyotrophic lateral sclerosis (ALS) is a devastating neurological disorder characterized by the degeneration of motor neurons and typically results in death within 3–5 years from onset. Familial ALS (FALS) comprises 5%–10% of ALS cases, and the identification of genes associated with FALS is indispensable to elucidating the molecular pathogenesis. We identified a Japanese family affected by late-onset, autosomal-dominant ALS in which mutations in genes known to be associated with FALS were excluded. A whole- genome sequencing and parametric linkage analysis under the assumption of an autosomal-dominant mode of inheritance with incomplete penetrance revealed the mutation c.2780G>A (p. Arg927Gln) in ERBB4. An extensive mutational analysis revealed the same mutation in a Canadian individual with familial ALS and a de novo mutation, c.3823C>T (p. Arg1275Trp), in a Japanese simplex case. These amino acid substitutions involve amino acids highly conserved among species, are predicted as probably damaging, and are located within a tyrosine kinase domain (p. Arg927Gln) or a C-terminal domain (p. Arg1275Trp), both of which mediate essential functions of ErbB4 as a receptor tyrosine kinase. Functional analysis revealed that these mutations led to a reduced autophosphorylation of ErbB4 upon neuregulin-1 (NRG-1) stimulation. Clinical presentations of the individuals with mutations were characterized by the involvement of both upper and lower motor neurons, a lack of obvious cognitive dysfunction, and relatively slow progression. This study indicates that disruption of the neuregulin-ErbB4 pathway is involved in the pathogenesis of ALS and potentially paves the way for the development of innovative therapeutic strategies such using NRGs or their agonists to upregulate ErbB4 functions.

Amyotrophic lateral sclerosis (ALS) is a devastating neurological disorder in which the degeneration of motor neurons leads to progressive weakness and wasting of limb, bulbar, and respiratory muscles. Familial ALS (FALS) comprises 5%–10% of ALS cases, and the remaining cases are simplex cases of ALS (SALS). To date, more than 20 genes have been shown to be associated with ALS,[1] and these account for 75% of FALS and 14% of SALS cases.[2] Mutations that are found in FALS-associated genes but that are also identified in individuals with SALS are considered mutations with reduced penetrance or de novo mutations. Further discovery of genes associated with FALS is indispensable

to elucidating the molecular backgrounds of both FALS and SALS.

Identification of genes associated with familial diseases has been accomplished through identification of the disease loci on the chromosomes by linkage analysis of large pedigrees and subsequent positional cloning of the genes. The majority of the FALS pedigrees, however, are not large and do not have multiple affected members as a result of the poor prognosis of the disease and the late age of onset, which makes it difficult to sufficiently narrow the candidate regions by linkage analyses and means that it takes a tremendous effort to identify the genes associated with FALS. The recent development of massively parallel

[1]Department of Neurology, Graduate School of Medicine, The University of Tokyo, Tokyo 113-8655, Japan; [2]Department of Computational Biology, Graduate School of Frontier Sciences, The University of Tokyo, Chiba 277-8561, Japan; [3]Comparative Genomics Laboratory, National Institute of Genetics, Shizuoka 411-8540, Japan; [4]Department of Medical Biochemistry and Genetics, University of Turku, Turku, 20014, Finland; [5]Turku Doctoral Programme of Biomedical Sciences, Turku, 20520, Finland; [6]Department of Neurology and Clinical Pharmacology, Ehime University Hospital, Ehime 791-0295, Japan; [7]Research Center, Centre Hospitalier Universitaire Sainte-Justine, Université de Montreal, Montreal, QC, H3T 1C5, Canada; [8]Department of Pathology and Cellular Biology, Université de Montréal, Montreal, QC H3T 1C5, Canada; [9]Department of Neurology, National Hospital Organization Ehime National Hospital, Ehime 791-0281, Japan; [10]Division of Neurology, First Department of Internal Medicine, Osaka Medical College, Osaka 569-8686, Japan; [11]Department of Neurology and Neuropathology and Brain Bank for Aging Research, Tokyo Metropolitan Geriatric Hospital and Institute of Gerontology, Tokyo 173-0015, Japan; [12]Department of Neurology, Brain Research Institute, Niigata University, Niigata 951-8520, Japan; [13]Department of Neuropathology, Institute for Medical Science of Aging, Aichi Medical University, Aichi 480-1195, Japan; [14]Department of Neurology, Nagoya University Graduate School of Medicine, Nagoya 466-8560, Japan; [15]Japanese Consortium for Amyotrophic Lateral Sclerosis Research; [16]Northcott Neuroscience Laboratory, ANZAC Research Institute, Sydney, New South Wales 2139, Australia; [17]Sydney Medical School, University of Sydney, New South Wales 2006, Australia; [18]Austrian School of Medicine, Macquarie University, Sydney, New South Wales 2109, Australia; [19]Department of Neurology, University of Massachusetts Medical School, Worcester, MA 01655-0318, USA; [20]Department of Oncology, Turku University Hospital, Turku 20521, Finland; [21]Montreal Neurological Institute, McGill University, Montreal, QC H3A 2B4, Canada; [22]Department of Neurology and Neurosurgery, McGill University, Montreal, QC H3A 2B4, Canada; [23]Medical Genome Center, The University of Tokyo Hospital, The University of Tokyo, Tokyo 113-8655, Japan
*Correspondence: tsuji@m.u-tokyo.ac.jp